Resonance pattern in electronic transmittance for two identical coupled random-dimer chains under different lead configurations

Tapas Mitra and Prabhat Kumar Thakur

S. N. Bose National Centre for Basic Sciences, DB 17, Sector 1, Salt Lake City, Calcutta 700064, India

Electronic transmittance vs energy for two identical coupled random-dimer chains is investigated within the Anderson tight-binding model. The electronic transmittance is calculated by using the Block recursion algorithm proposed by Godin and Haydock. The single-chain random-dimer result such as occurrence of band of nonscattered states is recovered for very small interchain hopping parameter. The transmittance vs energy curve shows a resonance pattern, which is highly sensitive to both interchain hopping and lead positions. Even for the moderate interchain hopping the band of nonscattered states gets modified by appearance of strong fluctuations or irregular dips leading to a new pattern for the transmittance vs energy curve.

I. INTRODUCTION

Electronic states in random potentials are localized both in one and two dimensions even for infinitesimally small disorder.[1(a)] However, in the past Azbel[1(b)] and others[1(c),18] have reported the existence of extended states appearing in the form of exponentially narrow resonances in electronic transmission through random potentials at energy points randomly positioned in the spectrum. In recent years much effort has been devoted to the study of electronic transport in disordered systems which have some kind of short-range correlation in the potential.[2–11] In these works the existence of extended states in a disordered potential in one dimension with a short-ranged spatial correlation is predicted, in contrast to the all-states-localized situation for a random potential without any spatial correlation.[1(a)] In this context many models have been proposed to describe some realistic situation, as one can have, for example, in the transport mechanism for conducting polymers[2–5] or quasi-one-dimensional (quasi-1D) superlattices,[8,12–15] etc. The simplest of these models is the random-dimer model (RDM) of Dunlap, Wu, and Phillips.[2] It has been shown by Wu and Phillips[3] that a single protonated strand of conducting polymer polyaniline can be described by the RDM. Recently, attempts have been made to describe the electronic transport mechanism in some superlattice structures by Kronig-Penney-type models for random-dimer potentials.[8] It has been realized that RDM's support a band of nonscattered states which can account for the enhanced conductivity in these materials.[3–5] It has been shown that a source of delocalization even in the dense defect limit arises from the single-impurity resonance effect, and eventually forms a broad resonance of finite width (where transmittance is unity) around the dimer defect resonance energy. However, the detailed numerical calculation by Datta, Giri, and Kundu[7] for finite concentrations of dimer defects have shown that the width is sensitive to the choice of site energies and concentration. In all these physically relevant systems, in which randomness as well as some short-ranged correlation is present, one hopes to have transport dominant only in one direction. Thus the result of the one-dimensional Hamiltonian is thought to be sufficient to describe the physical situation one observes in polyaniline or in other relevant systems. However, the idea of modeling a real system by coupled chains with small interchain coupling or by an effective single chain may break down in some situations. Wu and Phillips[3] think that the dynamics will be inherently two dimensional if the transverse hopping distance is comparable to the single-chain length. The effect of electron tunneling in the transverse direction may become important in general in many realistic quasi-1D systems.[12–15]

This motivated us to study electronic transport in a system of two coupled random chains with short-range correlation. We consider the short-range correlation within the RDM. As we will see, our investigation will throw some light on transport characteristics influenced by the interchain hopping contributions. The idea is to check, for small or moderate values of interchain hopping, whether the resonant features within a broad band are really preserved. Another possibility is that different localization-delocalization behavior may set in due to the same interchain tunneling but with different lead configurations.

II. MODEL OF TWO COUPLED RANDOM-DIMER CHAINS

Here we describe the electron motion in a two-coupled-chain geometry by an Anderson tight-binding Hamiltonian. The Hamiltonian can be written as

$$\hat{\mathbf{H}} = \sum_{n=-\infty}^{+\infty} (\mathbf{P}_n^\dagger \varepsilon_n \mathbf{P}_n + \mathbf{P}_n^\dagger \mathbf{V}_{n,n+1} \mathbf{P}_{n+1} + \mathbf{P}_{n+1}^\dagger \mathbf{V}_{n+1,n} \mathbf{P}_n),$$

(1)

where ε_n, $V_{n,n+1}$, and P_n are the following matrices with site and chain indices:

$$\varepsilon_{\mathbf{n}} = \begin{bmatrix} \epsilon_n^1 & t_c \\ t_c & \epsilon_n^2 \end{bmatrix},$$

$$\mathbf{V}_{\mathbf{n,n+1}} = \begin{bmatrix} t_{n,n+1}^1 & 0 \\ 0 & t_{n,n+1}^2 \end{bmatrix} = \mathbf{V}_{\mathbf{n+1,n}},$$

$$\mathbf{P_n} = \begin{bmatrix} \alpha_n \\ \beta_n \end{bmatrix}.$$

$\alpha_n^\dagger$ and $\beta_n^\dagger$ are creation operators in two chains, respectively.

The two chains have been considered to be identical. Thus here an arrangement of sites in a single chain is all that is necessary. We generate the random-dimer model by assigning the site energy to a pair, called a dimer, distributed randomly along the chain. The site energy ϵ_n^1 is selected from the value generated from a random number sequence $(0 < R < 1)$ in the following way: If $R < c$,

$$\begin{Bmatrix} \epsilon_n^1 = \epsilon_A \\ \epsilon_{n+1}^1 = \epsilon_A \end{Bmatrix},$$

while for, $R > c$,

$$\begin{Bmatrix} \epsilon_n^1 = \epsilon_B \\ \epsilon_{n+1}^1 = \epsilon_B \end{Bmatrix},$$

c being some fraction.

This is a quasi-1D system, where short-ranged correlation is due to the block of four impurity sites, and the interchain hopping t_c is considered to be finite in contrast to the single random-dimer chain where a pair of sites is occupied by the same species. The model of two identical coupled random-dimer chains simulates a quasi-1D wire, where the impurity atoms appear within a block in the host.

We focus our main interest in the regime $t_c \lesssim t$, which constitutes a different physically distinct regime as compared to the decoupled chain limit, i.e., $t_c \ll t$.

III. BLOCK RECURSION ALGORITHM

We employ the block recursion algorithm of Godin and Haydock to calculate quantum electronic transmittance. This method has proven to be numerically stable in 1D, 2D, and 3D systems.[16–18] The Hamiltonian of the sample is taken to be a tight-binding model with only nearest-neighbor overlaps nonzero. We attach M number of 1D incoming leads on one side of the sample, and M number of 1D outgoing leads on the opposite side of the sample. The leads are perfectly conducting, having a Hamiltonian of the form

$$H_L = V_L \sum_i \sum_j |i\rangle\langle j|. \tag{2}$$

V_L can be adjusted to make the lead bandwidth comparable to or larger than that of the sample. These leads support incoming and outgoing waves into and away from the sample.

The aim of the method is to calculate transmittance and reflectance (which are related to the square modulus of non-diagonal and diagonal elements of the $[S_{pq}]$ matrix, where p and q are lead indices) for the stationary state problem

$$\hat{H}|\Psi\rangle = E|\Psi\rangle. \tag{3}$$

In this method, a basis is calculated recursively in which the sample Hamiltonian becomes block tridiagonal, i.e., if we partition the sample Hamiltonian into matrix blocks of size $2M \times 2M$ then only diagonal and subdiagonal blocks are

nonzero. The lead Hamiltonian is kept unchanged. The first element $|\phi_1\rangle$ of this basis is chosen to be

$$|\phi_1\rangle = \begin{bmatrix} u_1^I \\ u_2^I \\ \vdots \\ u_M^I \\ u_1^O \\ u_2^O \\ \vdots \\ u_M^O \end{bmatrix}, \tag{4}$$

where u's refer to those orbitals of the samples where leads are attached. Here I and O refer to incoming and outgoing channels. Subsequent elements of the basis are generated from the following relations:

$$B_2^+|\phi_2\rangle = (\hat{H} - A_1)|\phi_1\rangle, \tag{5}$$

$$B_{n+1}^+|\phi_{n+1}\rangle = (\hat{H} - A_n)|\phi_n\rangle - B_n|\phi_{n-1}\rangle$$
$$\text{where} \quad n \geq 2. \tag{6}$$

If the original basis of the sample containing N orbitals was represented by N row vectors of size N, then the basis is represented by matrices of size $2M \times N$. A_n's and B_n's are $2M \times 2M$ matrices,

$$\begin{bmatrix} A_n = \phi_n^+ \hat{H} \phi_n \\ B_n = \phi_{n+1}^+ \hat{H} \phi_n \\ B_{1_{pq}} = \delta_{pq} V_L \end{bmatrix}.$$

The solution of the stationary-state problem in Eq. (1) is given by

$$|\Psi\rangle = \sum_n \psi_n |\phi_n\rangle. \tag{7}$$

The projections ψ_n's of the stationary-state solution $|\Psi\rangle$ into the basis $\{|\phi_n\rangle\}$ is calculated from the relation

$$\psi_n = X_n \psi_0 + Y_n \psi_1, \tag{8}$$

$$|\phi^0\rangle = \begin{bmatrix} u_1^0 \\ u_2^0 \\ \vdots \\ u_M^0 \\ u_{M+1}^0 \\ \vdots \\ u_{2M}^0 \end{bmatrix}, \tag{9}$$

where u^0's refer to the orbitals at M lead ends coupled to the sample via matrix element $V_L \cdot \psi^0$'s is the projection of Ψ into $|\phi^0\rangle$. X_n's and Y_n's are $2M \times 2M$ matrices calculated

by the same recursion relation that was used to calculate the basis, with EI replacing the Hamiltonian $\hat{H}$ and with the initial choices, $X_0=\hat{I}$, $Y_0=\hat{0}$, $X_1=\hat{0}$, and $Y_0=\hat{I}$. X's and Y's and $\hat{0}$ and $\hat{I}$ are $2M \times 2M$ matrices.

As the sample basis space is of rank N, our basis is spanned by $N/2M=p$ independent elements. This leads to the boundary condition

$$\psi_{p+1}=0. \tag{10}$$

The solution of Eq. (3) in the leads are Bloch waves of the form

$$\psi_L=\sum_m A \, \exp(\pm im\theta)|m\rangle, \tag{11}$$

where θ is the relative phase between the projections of ψ_L into the mth and $(m+1)$th site orbitals of the leads, and $\cos\theta=E/2V_L$. The second boundary condition comes from the known solution in the leads,

$$\psi_m=\begin{pmatrix} \exp(im\theta)+r_{1,1}\exp(-im\theta)+r_{1,2}\exp(-im\theta)+\cdots+r_{1,M}\exp(-im\theta) \\ \exp(im\theta)+r_{2,1}\exp(-im\theta)+r_{2,2}\exp(-im\theta)+\cdots+r_{2,M}\exp(-im\theta) \\ \vdots \\ t_{M+1,1}\exp(im\theta)+t_{M+1,2}\exp(im\theta)+\cdots+t_{M+1,M}\exp(im\theta) \\ t_{M+2,1}\exp(im\theta)+t_{M+2,2}\exp(im\theta)+\cdots+t_{M+2,M}\exp(im\theta) \\ \vdots \\ t_{2M,1}\exp(im\theta)+t_{2M,2}\exp(im\theta)+\cdots+t_{2M,M}\exp(im\theta) \end{pmatrix}, \tag{12}$$

m being 0 or 1.

$$\psi'_m=\begin{bmatrix} t_{1,M+1}\exp(-im\theta)+t_{1,M+2}\exp(-im\theta)+\cdots+t_{1,2M}\exp(-im\theta) \\ t_{2,M+1}\exp(-im\theta)+t_{2,M+2}\exp(-im\theta)+\cdots+t_{2,2M}\exp(-im\theta) \\ \vdots \\ t_{M,M+1}\exp(-im\theta)+t_{M,M+2}\exp(-im\theta)+\cdots+t_{M,2M}\exp(-im\theta) \\ \exp(im\theta)+r_{M+1,M+1}\exp(-im\theta)+r_{M+1,M+2}\exp(-im\theta)+\cdots+r_{M+1,2M}\exp(-im\theta) \\ \exp(im\theta)+r_{M+2,M+1}\exp(-im\theta)+r_{M+2,M+2}\exp(-im\theta)+\cdots+r_{M+2,2M}\exp(-im\theta) \\ \vdots \\ \exp(im\theta)+r_{2M,M+1}\exp(-im\theta)+r_{2M,M+2}\exp(-im\theta)+\cdots+r_{2M,2M}\exp(-im\theta) \end{bmatrix}, \tag{13}$$

m being 0 or 1.

$$\psi'_{N+1}=X_{N+1}\psi'_0+Y_{N+1}\psi'_1=0. \tag{14}$$

Here r stands for the reflection coefficient, and t stands for the transmission coefficient in Eqs. (12) and (13). If we now interchange the incoming and outgoing leads we obtain another set of boundary conditions.

From the boundary conditions written in expression (10) and (11)–(15), we obtain the expression for the S matrix:

$$S=\begin{pmatrix} \mathbf{r} & \mathbf{t} \\ \mathbf{t}' & \mathbf{r}' \end{pmatrix} = -[X_{N+1}+Y_{N+1}\exp(-i\theta)]^{-1}$$

$$\times[X_{N+1}+Y_{N+1}\exp(i\theta)]. \tag{15}$$

The total transmittance is given by

$$T=\sum_i \sum_o \left|\frac{t_{OI}}{2M}\right|^2 \tag{16}$$

and the total reflectance is given by $R=\sum_I\sum_{I'}|r_{II'}/2M|^2$. Here we have $R+T=1$ due to current conservation. Further-

more, as there is no applied magnetic field, the time-reversal symmetry holds good, and so $S_{ij}=S_{ji}$.

The relation between conductance and transmittance has been obtained in many contexts regarding both single-channel and multichannel situations, either from the Kubo formula or from the Landauer formula.[19]

IV. RESULTS AND DISCUSSION

In our calculations we have chosen a site energy corresponding to the lead Hamiltonian to be zero, while the intrachain hopping in the leads is unity and chosen to be the same as the intrachain hopping of the sample. The interchain hopping of the sample is considered to be small for $t_c \ll t$ values, and large when t_c becomes of the order of t values.

We have studied the total transmittance (T) for the two coupled random-dimer chains with the same hopping parameter t along the chains and different choices of the parameters ϵ, i.e., (ϵ_A, ϵ_B), and concentration c of dimer impurities in the chains. We first choose a set of parameters $\epsilon_A=0.5$, $\epsilon_B=0.25$, $c=0.10$, and $t_c=0.001$ for the calculation of transmittance for a wide range of energies, namely from -1.0 to 1.5 in units of hopping parameters in the lead
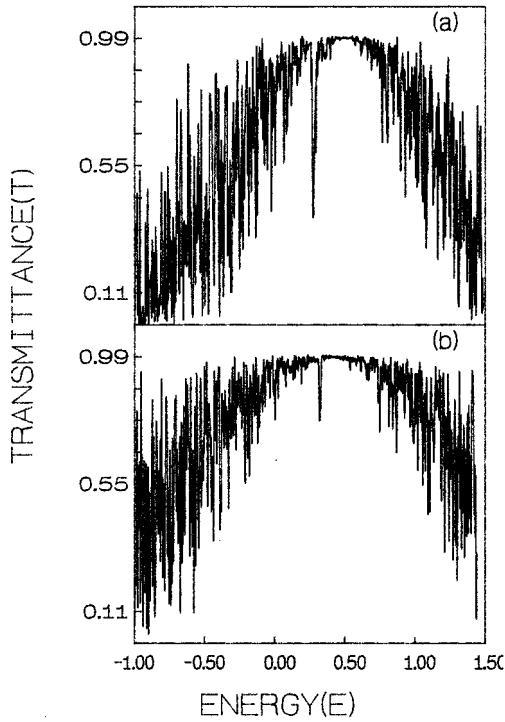
FIG. 1. (a) Transmittance (T) vs energy (E) for $\epsilon_A = 0.50$, $\epsilon_B = 0.25$, $c = 0.10$, $t_c = 0.001$, and $N = 3256$ sites. $t = 1.0$. (b) Transmittance (T) vs energy (E) for $\epsilon_A = 0.42$, $\epsilon_B = 0.30$, $c = 0.20$, $t_c = 0.001$, and $N = 3256$ sites. $t = 1.0$.

FIG. 2. Logarithm of the transmittance ($\ln T$) vs energy (E) for $\epsilon_A = 0.5$, $\epsilon_B = 0.25$, $c = 0.10$, $t_c = 0.35$, $t = 1.0$, $N = 2256$ (dashed), and $N = 3256$ (solid).

Hamiltonian. First we attach two decoupled 1D leads on either side along the direction of the sample length; that is, the calculation is done in the four-lead geometry. In Figs. 1(a) and 1(b) T vs energy (E) is plotted for the first set of parameters for a system size $N = 3256$ sites. One can clearly see that for a finite range of energy values around $E = 0.50$ the transmittance becomes almost flat, i.e., ($T \sim 1$), a wide region over which transmittance resonance is maintained. We can consider this value of t_c to be small enough to produce the single random-dimer chain result. This also suggests that the choice of our system size seems to be appropriate for studying delocalization or resonance aspects in such quasi-1D systems. It is also indicative of the fact that these are extended states of nonzero measure, which is at least true for such finite sample sizes.

We do the calculations for another set of parameters, i.e., $\epsilon_A = 0.42$, $\epsilon_B = 0.30$, $t_c = 0.001$, $c = 0.20$, and $N = 3256$ sites. The transmittance T vs energy plot for this case is shown in Fig. 1(b), clearly showing again the single-chain dimer result, i.e., the existence of nonscattered states for a range of energy values around $E = 0.42$.

Next we choose the interchain hopping parameter t_c to be comparatively large, to make the electron motion in the transverse direction significant so that transport characteristics dramatically change from the strictly 1D situation. We calculate the transmittance for $\epsilon_A = 0.5$, $\epsilon_B = 0.25$, $c = 0.10$, and $t_c = 0.35$, for two different system sizes $N = 2256$ and 3256 sites. In Fig. 2 the $\ln T$ vs E plot is shown for the two different sizes, respectively. One can hardly distinguish the two curves since the resonant features do not change much with the increase of system size. Here the $\ln T$ vs E plot
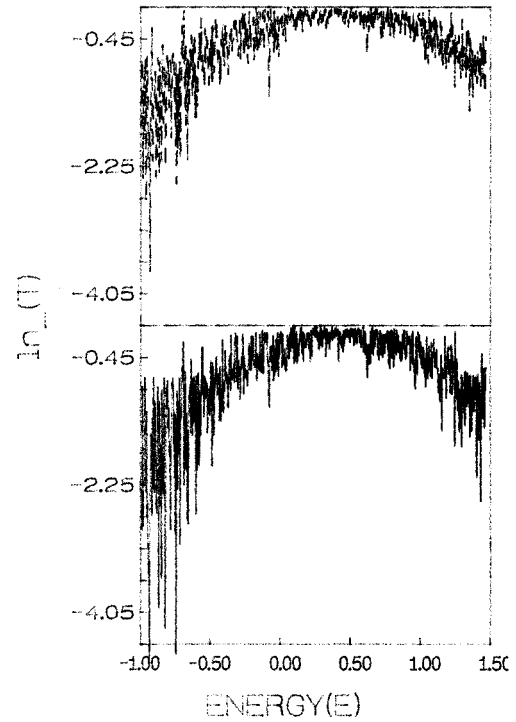
shows the growth of $\ln T$ from the left or right of the whole energy region concerned. It has a different delocalization nature for the states having $\ln T \sim 0$ than the nonscattered states one observes in Figs. 1(a) and 1(b). The regime of energies where $\ln T \sim 0$ corresponds to states with large localization lengths.

Now we go to a regime of transverse hopping, where the parameter $t_c = 0.125$, 0.25, and 0.50 for $\epsilon_A = 0.42$, $\epsilon_B = 0.30$, $c = 0.20$, and $N = 2256$ sites. Transmittance versus energy graphs have been shown, respectively, in Figs. 3(a), 3(b), and 3(c) for these parameters, and in the four-lead geometry as before. Here the input and output leads are attached to the ends along the chain direction. Note that we have also considered the $\ln T$ vs energy E plot here for finite chain coupling t_c. In this situation the motion of electrons in the transverse direction also becomes significant, and the total transmittance gives a clear signature of the combined interference effects due to the motion of electrons along the chain direction as well as in the transverse direction. Thus, with the increase of interchain hopping parameters between 0.1 to 0.5, the overall resonance features in the transmittance drastically changes to a fluctuating pattern over all energy scales. In the resonant region (where $\ln T \sim 0$) it shows almost uniform fluctuations. Thus here for a wide range of energies the delocalization of states is manifested as before, with an underlying fluctuation pattern in contrast to the extended states (transmittance is flat and $T \to 1.0$) in the single random-dimer chain. Now we will analyze situations where electronic transmittance has been calculated in different measurement geometries, and where first, the input and output leads are considered to be at the corners of the sample, and second, a situation where the leads are on the two sides
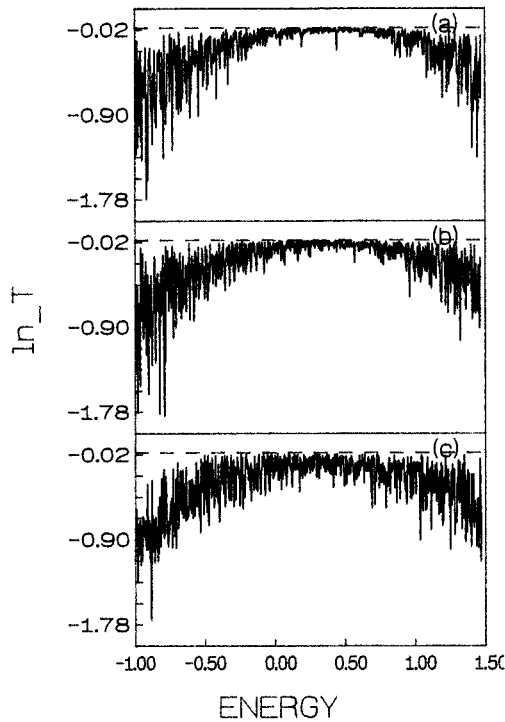
FIG. 3. (a) Logarithm of the transmittance (ln$T$) vs energy (E) for $\epsilon_A=0.42$, $\epsilon_B=0.30$, $t_c=0.125$, $c=0.20$, and $N=2256$ sites. (b) Same plot, but for $t_c=0.250$. (c) Same plot, but for $t_c=0.50$.
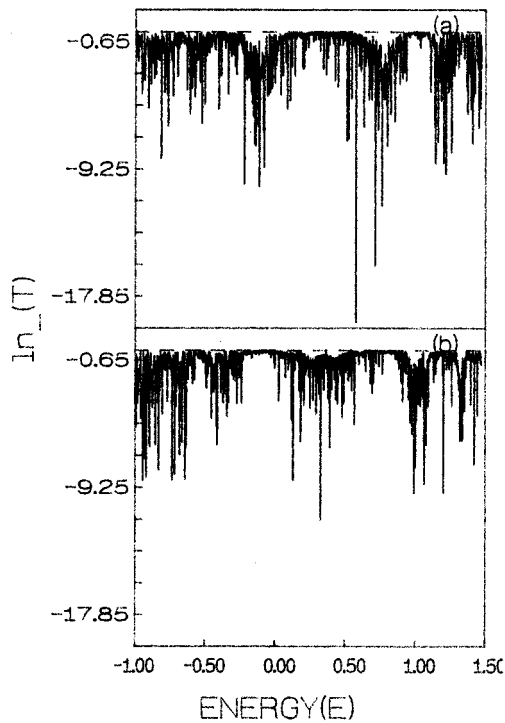
FIG. 5. (a) Logarithm of the transmittance (ln$T$) vs energy (E) for $\epsilon_A=0.50$, $\epsilon_B=0.25$, $t_c=1$, and $c=0.10$ in a four-lead geometry. (b) Same plot as in (a) but for $\epsilon_A=0.42$, $\epsilon_B=0.30$, $t_c=1.0$, and $c=0.20$.

FIG. 4. (a) Logarithm of the transmittance (ln$T$) vs energy for corner leads attached to the sample for chain parameters as in Fig. 3(a) but for $t_c=0.045$ and $N=3256$ sites. (b) Same plot as in (a) but for the situation where leads are attached on the left and right ends of the lower chain.
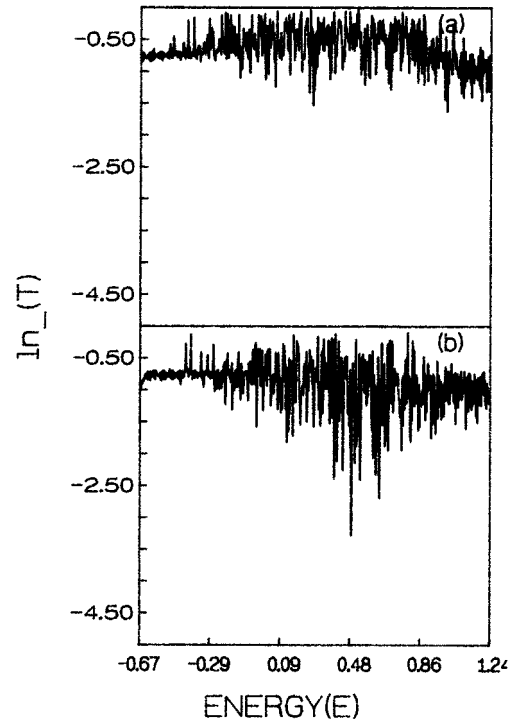
of a single chain. We see how resonance features may become different in such different input-output lead configurations. In Fig. 4(a) a transmittance vs energy plot has been shown when input and output leads are at the corners and the interchain coupling t_c is finite; here we choose $t_c=0.045$. However, the other chain parameters are the same as in Figs. 3(a)–3(c), and for the system size $N=3256$ sites. Similarly, Fig. 4(b) shows the same plot but with input-output leads attached to the left and right sides of the lower chain, respectively, for the same set of parameters as in Fig. 4(a). If we compare Figs. 4(a) and 4(b) the distinct nature of the localization-delocalization aspects have been reflected through the ln$T$ vs E curve for the same sample, but with different lead configurations. In both figures the ln$T$ vs E plot gives a clear signature for regions of many delocalized states as well as sharp dips which occur in an irregular fashion. As one increases t_c, more and more dips appear in an irregular fashion in the vicinity of states having ln$T\sim0$. This is attributable to the underlying quantum interference effects under different lead configurations.

Next we go over to a situation where the interchain coupling t_c becomes the same as the intrachain coupling t. Results for ln$T$ vs energy E have been shown in Figs. 5(a) and 5(b) for two different set of parameters. A strongly fluctuating pattern emerges in this situation as the interchain coupling t_c becomes the same as the intrachain coupling t. Since more dips appear in this situation, electronic states seem to become more localized at many energy points, as compared to previous cases where t_c is less than t.

Thus, as we increase the coupling t_c shown in the Figs. 3(a)–3(c), 4(a), 4(b), 5(a), and 5(b), one can clearly observe

a significant amount of fluctuations appearing in the regime of delocalized states in the previous case. As the fluctuations grow with increasing coupling t_c, one can see that localization and delocalization become of competing natures at many of the energy values and in their vicinity. Thus localization and delocalization of electronic states in the coupled-chain case have different resonant features altogether than those in a single chain of same length.

V. SUMMARY AND CONCLUSION

In this electronic transport calculation an attempt has been made to explore the possibility of the existence of delocalized or resonance states in two coupled chains with random-dimer-type short-range correlation in the on-site potential. Calculation of the transmittance for the system has been carried out numerically using the block recursion algorithm of Godin and Haydock for the nearest-neighbor Anderson tight-binding model. Calculation is done for different interchain couplings, while the hopping along the chain is kept constant. The calculation shows a fluctuating pattern for the transmittance, in contrast to the single-chain case, when one observes the signature of extended states without any fluctuation. The pattern for the four-lead situations has resonance features ($\ln T \sim 0$) over a wide range of energies, while for other lead configurations it has a different signature altogether. This is reminiscent of typical quantum interference effects which may originate from the arrangement of input and output leads attached in a particular fashion to the sample. We think that essential features of our results also remain valid where the two chains have different configurations with same chain parameters.

This calculation highlights the different signatures of typical resonance features in the electronic states in the two coupled-chain cases with wide ranges of couplings for different lead configurations. The analysis draws serious attention to issues such as whether interchain tunneling effects are really important when dealing with electronic transport properties in such realistic systems with both finite and infinite chain lengths. We do hope that the model of coupled random-dimer chains may provide some insight into modeling more realistic systems where short-ranged order may be present in the same or different forms in a quasi-1D disordered wire or other polymeric system.

[1] (a) P. W. Anderson, Phys. Rev. **109**, 1492 (1958); T. V. Ramakrishnan and P. A. Lee, Rev. Mod. Phys. **57**, 287 (1985) and references therein; (b) M. Ya Azbel and P. Soven, Phys. Rev. B **27**, 831 (1983); M. Ya Azbel and P. Soven, Phys. Rev. Lett. **49**, 751 (1982); (c) J. B. Pendry, J. Phys. C **20**, 733 (1987); C. Basu, A. Mookerjee, A. K. Sen, and P. K. Thakur, J. Phys. Condens. Matter **3**, 9055 (1991).

[2] D. H. Dunlap, H. L. Wu, and P. Phillips, Phys. Rev. Lett. **65**, 88 (1990).

[3] H. L. Wu and Philip Phillips, Phys. Rev. Lett. **66**, 1366 (1991).

[4] H. L. Wu, W. Goff, and P. Phillips, Phys. Rev. B **45**, 1623 (1992).

[5] P. Phillips, H. L. Wu, and D. Dunlap, Mod. Phys. Lett. B **4**, 1249 (1990); D. H. Dunlap, K. Kundu and P. Phillips, Phys. Rev. B **40**, 10 999 (1989).

[6] S. Sil, S. N. Karmakar, R. K. Moitra, and A. Chakraborty, Phys. Rev. B **48**, 4192 (1993) .

[7] P. K. Data, D. Giri, and K. Kundu, Phys. Rev. B **47**, 10 727 (1993).

[8] Angel Sanchez, Phys. Rev. B **49**, 147 (1994); C. Basu and P. K. Thakur, Physica A **217**, 289 (1995).

[9] D. Giri, P. K. Datta, and K. Kundu, Phys. Rev. B **48**, 14 113 (1993).

[10] S. Gangopadhyay and A. K. Sen, J. Phys. Condens. Matter **4**, 9939 (1992).

[11] C. M. Soukoulis, M. J. Velgakis, and E. N. Economu, Phys. Rev. B **50**, 5110 (1994).

[12] M. Hilke, J. Phys. A **27**, 4773 (1994).

[13] H. Ducker, M. Struck, Th. Koslowski, and W. Von Niessen, Phys. Rev. B **46**, 13 078 (1992).

[14] S. Stafstrom, Phys. Rev. B **51**, 4137 (1995).

[15] V. N. Prigodin and K. B. Efetov, Phys. Rev. Lett. **70**, 2932 (1993).

[16] T. J. Godin and Roger Haydock, Phys. Rev. B **38**, 5237 (1988); C. Basu, A. Mookerjee, A. K. Sen, and P. K. Thakur, J. Phys. Condens. Matter **3**, 6041 (1991).

[17] I. Dasgupta, T. Sen, and A. Mookerjee, J. Phys. Condens. Matter **4**, 7865 (1992).

[18] I. Dasgupta, T. Saha, and A. Mookerjee, Phys. Rev. B **50**, 4867 (1994).

[19] M. Buttiker, Y. Imry, R. Landauer, and S. Pinhas, Phys. Rev. B **31**, 6207 (1985); R. Landauer, Philos. Mag. **21**, 863 (1970); D. S. Fisher and P. A. Lee, Phys. Rev. B **23**, 6851 (1981).